

ReS₂ on GaN Photodetector Using H⁺ Ion-Cut Technology

Xinke Liu, Jie Zhou, Jiangliu Luo, Hangning Shi, Tiangui You, Xin Ou, Venkatadivakar Botcha, Fengwen Mu, Tadatomo Suga, Xinzhong Wang, and Shuangwu Huang*



Cite This: *ACS Omega* 2023, 8, 457–463



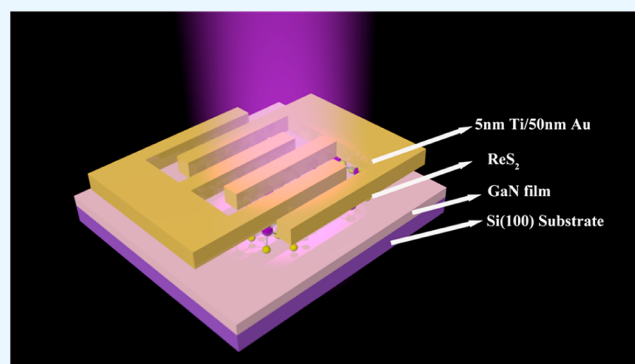
Read Online

ACCESS |

Metrics & More

Article Recommendations

ABSTRACT: The wafer-scale single-crystal GaN film was transferred from a commercial bulk GaN wafer onto a Si (100) substrate by combining ion-cut and surface-activated bonding. Well-defined, uniformly thick, and large-scale wafer size ReS₂ multilayers were grown on the GaN substrate. Finally, ReS₂ photodetectors were fabricated on GaN and sapphire substrates, respectively, and their performances were compared. Due to the polarization effect of GaN, the ReS₂/GaN photodetector showed better performance. The ReS₂/GaN photodetector has a responsivity of 40.12 A/W, while ReS₂/sapphire has a responsivity of 0.17 A/W. In addition, the ReS₂/GaN photodetector properties have reached an excellent reasonable level, including a photoconductive gain of 447.30, noise-equivalent power of 1.80×10^{-14} W/Hz^{1/2}, and detectivity of 1.21×10^{10} Jones. This study expands the way to enhance the performance of ReS₂ photodetectors.



INTRODUCTION

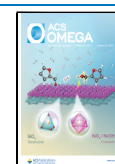
In the past decade, two-dimensional materials represented by graphene have attracted extensive attention due to their unique physical and chemical properties, such as ultra-high carrier mobility, good mechanical properties, and chemical stability.^{1–4} However, it has no band gap because of the semi-metallic properties of graphene. It is difficult to obtain a wide band gap through physical or chemical modulation, which limits its application in the field of optoelectronics, such as field effect transistors and photodetectors.^{5,6} With the deepening of research and application, transition metal dichalcogenides (TMDs) have gradually entered the vision of researchers. They possess properties similar to graphene but with tunable band gaps. Monolayer TMDs have a “sandwich” structure composed of two layers of chalcogen elements and a layer of transition metal atoms, and the layers are combined by weak van der Waals forces.³ Among TMDs, ReS₂ has become a research hotspot because of its unique physical structure and properties.^{7–10} ReS₂ has a unique twisted 1T phase crystal structure. Compared with traditional TMDs, ReS₂ has distinctive properties: first, ReS₂ is a direct band gap semiconductor from bulk material to monolayer material, in which the band gap is 1.35 eV in bulk and rises to 1.43 eV in monolayer. This makes ReS₂ potentially useful as a saturable absorber and photoelectrode material in optics and photoelectron chemistry.^{11–13} Second, it has been proved theoretically and experimentally that the optical and electrical properties of bulk ReS₂ and monolayer ReS₂ are almost identical.¹⁴ This allows researchers to study the microphysical properties of

ReS₂ without being limited by the size of the material and the number of layers. Then, ReS₂ shows strong in-plane anisotropy.¹⁵ Because of this property, ReS₂ can be used to fabricate polarization-dependent photodetectors, which can detect various directions of linearly polarized light in multi-channel optical communication.^{16–18} Finally, compared with black phosphorus with properties similar to ReS₂, ReS₂ has extreme environmental stability and does not need to pass specific protective gas or passivate the prepared material during the preparation and application process, significantly reducing the time, and labor costs in preparation and application are eliminated. In summary, we believe that ReS₂ has a vital research and application value. However, the growth and preparation method of layered ReS₂ is not yet perfect and immature.¹⁹ The characterization of the photoelectric properties of ReS₂ photodetectors is still in the theoretical stage, which lacks experimental support, and many critical optical parameters have not been revealed. Therefore, it is essential to carry out systematic research on ReS₂ photodetectors. Currently, large-area ReS₂ films can be obtained by chemical vapor deposition (CVD), but the choice of substrate is a crucial parameter. Gallium nitride (GaN) has now become the

Received: August 8, 2022

Accepted: November 21, 2022

Published: December 20, 2022



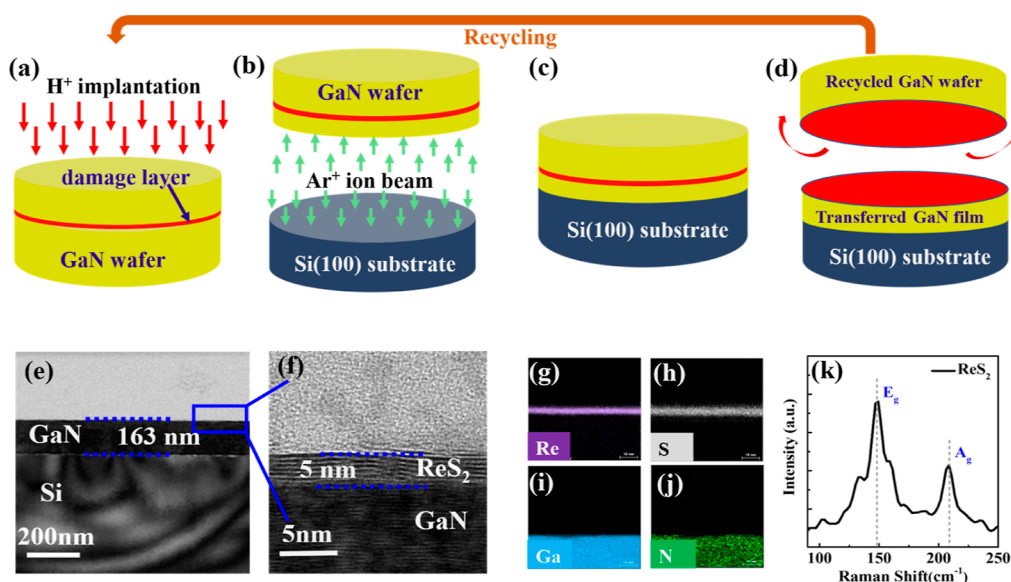


Figure 1. Process flow for processing GaN using the ion-cut technique. (a) Implanting H^+ into the bulk GaN wafer; (b) modified surface-activated bonding of GaN wafer and Si (100) wafer; (c) wafer bonding; and (d) removing the residual layer. (e) TEM image of the ReS_2 /GaN structure; (f) TEM image of ReS_2 ; EDS scan result of (g) Re element, (h) S element, (i) Ga element, and (j) N element of the sample; and (k) Raman spectrum of ReS_2 .

substrate of choice for the growth of most of the 2D materials. Since the production technology of GaN has improved, the supply of gallium nitride wafers in the market has gradually increased. However, the price of gallium nitride wafers is still high. If it is desired to grow ReS_2 thin films on GaN wafers, reducing manufacturing costs is a top priority. In 2020, Shi et al. used H ion-cut technology to obtain nanometer-thick GaN wafer thin films.²⁰ The sliced, bulk GaN wafers can be recycled and reused, which is beneficial in reducing costs. The Ga–N bonds of wurtzite GaN exist in two directions: parallel to the c -axis and non-parallel to the c -axis, which makes the bond strength and length of different Ga–N bonds different, and the bond along the [0001] direction is slightly longer. Therefore, this crystal structure causes the original cell's positive and negative charge centers not to coincide to form an electric dipole moment. The existence of the electric dipole moment generates a built-in electric field inside the crystal and spontaneous polarization characteristics.²¹ Due to this polarization effect, a strong electron–phonon interaction occurs between GaN and ReS_2 , which affects the optical properties of ReS_2 . Therefore, in this work, ReS_2 would be grown on GaN wafers processed by ion-cut technology and fabricated into photodetectors. This will be an exciting and meaningful study.

In this work, ion-cut technology transferred the wafer-scale single-crystalline GaN film from a commercialized bulk GaN wafer onto Si (100) substrate. Then, multilayer ReS_2 was grown on a GaN wafer by the CVD method to form the van der Waals heterostructure. Raman spectroscopy and transmission electron microscopy (TEM) were carried out on ReS_2 /GaN to verify the material quality. An integrated photodetector was fabricated by depositing electrodes using photolithography and thermal evaporation, followed by a lift-off process. The electrical measurements of the photodetectors were fully characterized, and first-principles calculations on ReS_2 and GaN were also out to explain the improvement of device performance.

EXPERIMENTAL DETAILS

Growth Materials and Preparation Devices. A wafer-scale single-crystalline GaN film was transferred from a commercialized bulk GaN wafer onto Si (100) substrate by combining ion-cut and surface-activated bonding. Then, GaN on Si (100) wafer was successfully washed and cleaned in an ultrasonic bath with acetone, isopropanol, and deionized water, followed by a blow dry with N_2 gas. Later, multilayer ReS_2 films were grown on GaN and sapphire substrates at the 750 °C by a CVD system (CVD-12IIH-3Z/G, TIANJING ZHONGHUAN FURNACE Corp., China). Rhenium trioxide powder and sulfur powder were precursors, and argon gas was the carrier gas with a flow velocity of 60 sccm. The required electrode arrays were obtained on the samples by UV lithography. Then, Ti (5 nm)/Au (50 nm) was plated on the sample as electrodes by the thermal evaporation technology and stripping process.

Materials and Electrical Characterizations. The Confocal Renishaw system was used to characterize the Raman spectroscopy for the relevant samples. The excitation wavelength of the system is 514.5 nm, and the power is 0.25 mW. The equipment used for transmission electron microscopy (TEM) testing is America FEI-Titan Cubed Themis G2 300, and its related equipment is carried out by energy-dispersive spectroscopy (EDS) analysis. A Keithley 4200-SCS semiconductor analyzer is used to test the electrical performance of photodetectors, including I – V characteristics and I – T characteristics.

First Principles Calculation. The theoretical calculations were performed through the Vienna ab initio simulation package (VASP) code based on the density functional theory (DFT). The Perdew–Burke–Ernzerhof version of the generalized gradient approximation (PBE-GGA) was used to calculate the exchange–correlation contributions to the total energy. The electron–ion interactions were described by the projector-augmented wave pseudopotentials (PBE). The energy cutoff was set to 500 eV. For the Brillouin zone integration, a $3 \times 3 \times$

1 Monkhorst–Pack k -point mesh was used for structure optimization, and a denser $5 \times 5 \times 1$ mesh was applied for the electronic property calculation. The convergence criteria were set to 10^{-3} and 10^{-5} eV for the atomic force and energy, respectively. The DFT-D3 approach was adopted to describe the Van der Waals interaction.

RESULTS AND DISCUSSION

In this work, a 2 in. wafer-scale single-crystalline GaN film was transferred from a commercialized bulk GaN wafer onto Si (100) substrate by combining ion-cut and surface-activated bonding. The cutting process of GaN is shown in Figure 1a–d. Bulk GaN wafer was first processed by H ion implantation. GaN and Si (100) wafer was then surface-activated using an Ar ion beam. The activated wafers were bonded under high pressure. Finally, the sample was annealed at 450 and 800 °C and was polished by chemico-mechanical polishing (CMP). The excess GaN wafers were recycled for recycling. Then, multilayer ReS₂ films were grown on a GaN wafer by CVD. To obtain the growth quality information of the sample, TEM and EDS tests were performed on this structure. The results are shown in Figure 1e,f. Above the Si (100) substrate is a 163 nm thick GaN thin film. Due to the high bonding strength of the modified surface-activated bonding, the GaN/Si heterobonding structure is thermally stable during the annealing process of preparation. Seven layers of the ReS₂ film were deposited on the upper surface of GaN, and the thickness is about 5 nm. The characteristic X-rays emitted by different elements have different energies and wavelengths, which can help us quickly determine the material's elemental composition. Figure 1g–j shows the element composition of the material and also reflects the relative position of the element material. From the results of EDS, ReS₂ was grown uniformly on the GaN wafer. Next, the two-dimensional material of the surface was characterized. Raman spectroscopy can detect the molecular vibration information of materials to analyze the properties of materials qualitatively. As shown in Figure 1k, strong characteristic peaks can be observed at positions 149.31 and 200 cm⁻¹, indicating that the two-dimensional material is ReS₂.^{16,22}

In order to study the effect of the GaN substrate on ReS₂, Vienna ab initio simulation package (VASP) was used for material modeling and calculating material properties. The result is shown in Figure 2a. The crystal parameters of the fully optimized wurtzite GaN ($a = b = 3.216$ Å; $c = 5.234$ Å) and two dimensional ReS₂ ($u = 6.389$ Å; $v = 6.495$ Å) show good

alignment with the experimental result. An enlarged 2×2 GaN(0001) supercell slab was used to contact the ReS₂ monolayer with the lattice mismatch of less than 2% in the X and Y directions. Besides, a 15 Å vacuum layer was applied in the Z direction to avoid the impact of image interaction. As the exposed GaN(0001) face is an asymmetry and polarized surface, both sides of the GaN contact situation are considered. For the GaN layer, unsaturated Ga or N atoms from the bottom surface are passivated by the pseudo hydrogen with the formal charge of 1.25 and 0.75, respectively. For the entire heterostructure, only the pseudo hydrogen and the bottom of GaN are fixed to mimic the bulk GaN. The final stacking pattern of the ReS₂/GaN heterostructure is determined through a relative movement of the adjacent GaN and ReS₂ layers to find a local energy minimum configuration. Figure 2a reflects the panner average charge difference of the ReS₂/GaN heterostructure. A dramatic charge difference fluctuation occurs at the contact interface of GaN and ReS₂. Since GaN is a spontaneously polarized material, the polarization effect causes polarization charges at the interface of GaN,^{23,24} and there is a strong electronic interaction with ReS₂, which profoundly affects the material properties of ReS₂; this phenomenon has been found in the study of MoS₂.^{2,25} In order to verify the photoelectric property change of ReS₂, the optical absorbance was tested on ReS₂/GaN and ReS₂/Sapphire samples, respectively. The result is shown in Figure 2b. Sapphire is not a spontaneously polarized material, and there is no polarization effect. In the visible light region, the optical absorption of ReS₂ on sapphire is smaller than that of ReS₂ on GaN, which indicates that ReS₂ significantly improves the optical absorption under the influence of the polarization effect of GaN.

Figure 3a,e exhibits an optical image and 3D model structure of a multilayer ReS₂ photodetector fabricated on a GaN substrate, respectively. The figure shows a cross-fingered electrode pattern. This design effectively increases the contact area between ReS₂ and the metal. Also, the electrode was composed of Ti (5 nm)/Au (50 nm). When the metal and semiconductor material come into contact, the band of the semiconductor at the interface is bent. Also, a Schottky barrier is created that acts as a high wall to stop the flow of electrons from the semiconductor into the metal. The energy bands are shown in Figure 3b,c. The presence of an obstacle results in a sizeable interfacial resistance, and the energy of electrons must be higher than this barrier to cross it into the metal. Here, low work function metals (such as Ti and Au) were chosen to form electrode contact points. This allows the device to perform well, including efficient carrier transport and interface contact. In this work, GaN and sapphire substrates were used to grow ReS₂, finish the fabrication of photodetectors, and test electrical properties. The test results are shown in Figure 3e,f. Sapphire is a kind of non-spontaneously polarized material with no polarization effect. Therefore, the sample can be used as a control group of GaN to explore the impact of the polarization effect of GaN on the performance of photodetectors. Figure 3e,f reflects the variation trend between the current (I) and voltage (V) plotted by the two devices under incident light at incident power of 2.163, 3.890, and 5.647 μW and dark. The figures show that the photodetectors can obtain a larger current under ample incident power, and the current increases gradually with the voltage increase. The current values for the ReS₂/GaN device are 1.62 and 220.20 μA at 10 V, which correspond to the dark environment and the 365 nm

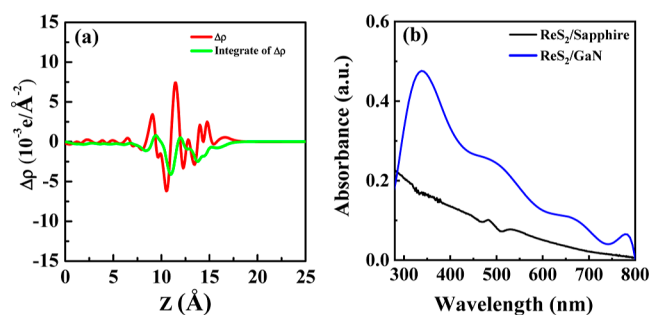


Figure 2. (a) Panner average charge difference of the ReS₂/GaN heterostructure; (b) because of the polarization effect of GaN, the absorption coefficient of ReS₂ improves obviously in the visible region.

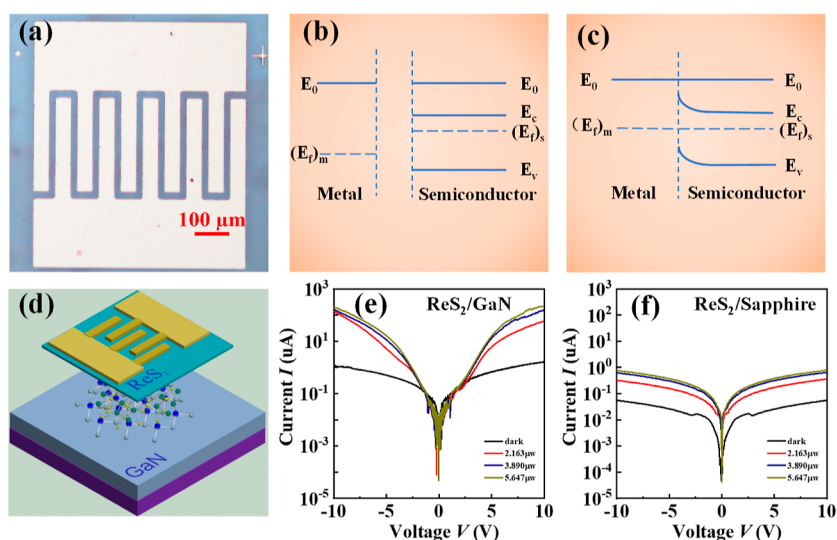


Figure 3. (a) Optical image of the ReS₂/GaN photodetector; (b,c) energy band diagram before contact and after contact for a metal–semiconductor; (d) 3D model structure of the ReS₂/GaN photodetector; and (e,f) current versus incident power curve of the ReS₂/GaN photodetector and ReS₂/Sapphire photodetector illuminated by 365 nm wavelength light.

wavelength lighting environment, respectively. The phenomenon that the photodetector gets a huge current boost under light is mainly due to the internal photoelectric effect of ReS₂. Electrons in the valence band absorb the incident photon energy and are then excited to the conduction band. So, a free movement electron is produced in the conduction band, and the valence band leaves a hole. The holes can be considered positive charge carriers that move freely in the valence band. Therefore, when the incident photons are excited in the semiconductor's valence band and conduction band, the photogenerated electron–hole pairs will change the conductivity of the semiconductor.^{26–28} At the same time, the charge carriers in the electrode region diffuse and reduce the barrier height. This is one of the reasons why the photocurrent increases.²⁹ Under the same conditions as above, the dark current and light current of the ReS₂/sapphire device were down significantly, reaching 0.05 and 0.79 μA, respectively. These values are significantly lower than those of the ReS₂/GaN device. To characterize the device's capability, the photocurrent I_{ph} is obtained by the following relationship.

$$I_{ph} = |I_{light}| - |I_{dark}| \quad (1)$$

where I_{light} and I_{dark} are currents under illumination and darkness, respectively. As can be seen from Figure 3e,f, when the effective power is 5.647 μW, the photocurrent of the ReS₂/GaN device is 218.58 μA, while the ReS₂/sapphire device is 0.74 μA. This is almost 295 times the ReS₂/sapphire device. To further illustrate the performance parameters of the devices, the responsivity R and photoconductive gain G are calculated according to the following formula

$$R = I_{ph}/P_{in} \quad (2)$$

and

$$G = (I_{ph}/P_{abs})/(h\nu/q) \quad (3)$$

where P_{abs} is the absorption power, defined as $P_{abs} = \mu P_{in}$. μ is the absorption rate. P_{in} is the effective power of the incident light, which is normalized by the equation $P_{in} = \text{power density} \times \text{active area}$. h is the Planck constant, ν is the incident laser frequency, and q is the elementary charge. The optical

responsivity R and photoconductive gain G of the ReS₂/GaN and ReS₂/sapphire device as a function of the effective power are shown in Figure 4a,b at 365 nm wavelength under 10 V

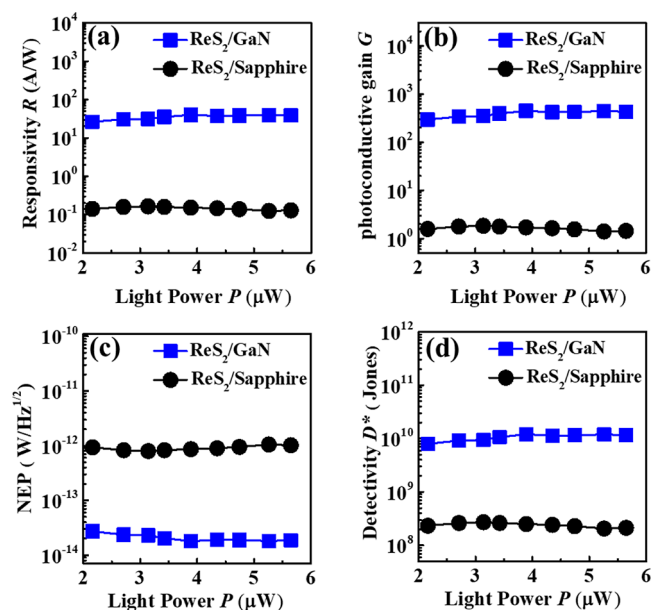


Figure 4. Device performance changes of two types of ReS₂ photodetectors, which were measured at a wavelength of 365 nm. The performance of the ReS₂ photodetectors varies with the change of the incident power, including (a) responsivity, (b) photoconductive gain, (c) noise equivalent power, and (d) normalized detectivity.

bias voltage. As shown in Figure 4a, when the responsivity R of the ReS₂/GaN device reaches the highest value of 40.12 A/W, the ReS₂/Sapphire device can reach 0.17 A/W, which is 236 times as much the ReS₂/Sapphire device. In addition, it can be observed that the responsivity of the ReS₂/GaN device increases before 3.89 μW and gradually decreases after that. This is because under 3.89 μW light irradiation, the stimulated absorption of electrons has reached saturation.^{30–32} Figure 4b

Table 1. Comparisons of Essential Performance Parameters of the ReS₂/GaN Photodetector with Recently Developed 2D Photodetectors

photodetector	R (A/W)	D* [Jones]	response time [s]	year	reference
ReS ₂ /GaN	40.1 (365 nm)	1.21 × 10 ¹⁰	0.01	2022	This work
ReS ₂ /sapphire	0.17 (365 nm)	2.72 × 10 ⁸	4.53	2022	This work
ReS ₂ bilayer film	0.004 (500 nm)		≈1.0	2016	8
ReS ₂ hexagon	604		0.002	2016	8
ReS ₂	0.22 (532 nm)		325.3 × 10 ⁻⁶	2021	12
MoS ₂ /GaN	172.12 (280 nm)			2019	25
	17.5 (405 nm)				
MoS ₂ /AlN	2.97 (365 nm)	1.71 × 10 ⁹		2021	2
NiO/GaN	0.15 (365 nm)		0.038	2018	33

demonstrates that the photoconductive gain increases from 1.84 for the ReS₂/Sapphire device to 447.30 for the ReS₂/GaN device. This means that the ReS₂/GaN device produces more photocarriers. To understand the detection capability of the photodetector, the noise equivalent power (NEP) and the normalized detectivity (D^*) are shown in Figure 4c,d. NEP is calculated by the following formula

$$\text{NEP} = (2qI_{\text{dark}}\Delta f)^{1/2}/R \quad (4)$$

where f is the bandwidth, here $\Delta f = 1$, only the shot noise in the current density is considered. NEP represents the ability of photodetectors to detect weak signals. D^* can be obtained by reciprocal processing and normalization of NEP. The photodetectors with a higher D^* value have better detection ability. D^* is calculated by the following formula

$$D^* = A^{1/2}/\text{NEP} \quad (5)$$

where A is the device effective working area. As the reciprocal of NEP, the larger the value of D^* , the higher the detection capability. Figure 4c,d shows the comparison of the noise NEP and D^* of ReS₂/Sapphire and ReS₂/GaN devices. By contrast, the lowest NEP = 1.80×10^{-14} W/Hz^{1/2} and the highest $D^* = 1.21 \times 10^{10}$ Jones were obtained in the ReS₂/GaN devices at 365 nm, which were 44 times lower and 44 times higher than the ReS₂/Sapphire devices, respectively. Table 1 illustrates the comparisons of essential performance parameters of the ReS₂/GaN photodetector with recently developed 2D photodetectors.

The reproducibility and speed of photodetectors can be understood via the measured I - T curves with a periodic on/off lighting. Figure 5a,b shows the photocurrent as a function of time using 365 nm light for the ReS₂/GaN device and ReS₂/

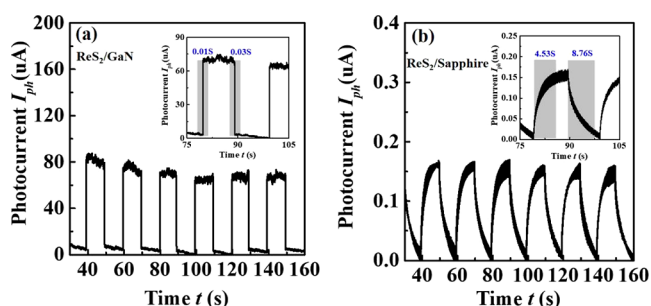


Figure 5. Occurrence of photocurrent in repeated dark and light environments. Photocurrent vs time curve of (a) ReS₂/GaN and (b) ReS₂/sapphire at 365 nm illumination. The corresponding rise time and fall time are shown in the inset.

Sapphire device. In the test of the I - T curve, the applied bias was set as 10 V, and the scanning time was set as 160 s. A computer-controlled light shutter was used to periodically block the light to the ReS₂ photodetector (illumination 20 s, darkness 20 s). The results show that the fast and uniform photocurrent increases and decreases periodically by controlling the light shutter with and without light. At first, there is almost no photocurrent response in the dark state. Then, when light hits the electrodes, a fast-responding photocurrent is generated on all the electrodes. Finally, the photocurrent gradually stabilizes. Consequently, the I - T curves reflect the photodetectors' long-term stability and high-performance reliability. In this research, a photodetector's rise time and fall time is defined as the time required to increase from 10 to 90% and decrease from 90 to 10% of the maximum photocurrent. Illustrations of Figure 5a,b showed the rise and fall times of the ReS₂/GaN device and ReS₂/Sapphire device, respectively. The rise times are estimated as 0.01 s for the ReS₂/GaN device and 4.53 s for the ReS₂/Sapphire device. The fast response of the former is attributed to ReS₂ itself with a direct band gap on the one hand, and the polarization effect of GaN enhances the optical properties of ReS₂ on the other hand.

CONCLUSIONS

In conclusion, we have successfully transferred the wafer-scale single-crystal GaN film from a commercial bulk GaN wafer onto a Si (100) substrate by combining ion-cut and surface-activated bonding. Also, uniform and large wafer size multilayer ReS₂ was satisfactorily grown on the GaN substrate. Finally, we fabricated ReS₂ photodetectors on GaN and sapphire substrates and compared their performances. Due to the polarization effect of GaN, the ReS₂/GaN photodetector showed better performance. The ReS₂/GaN photodetector has a responsivity of 40.12 A/W, while ReS₂/sapphire has a responsivity of 0.17 A/W. In addition, other ReS₂/GaN photodetector properties have reached a reasonable level, including a photoconductive gain of 447.30, NEP of 1.80×10^{-14} W/Hz^{1/2}, and detectivity of 1.21×10^{10} Jones. This study expands the way to enhance the performance of ReS₂ photodetectors.

AUTHOR INFORMATION

Corresponding Author

Shuangwu Huang – College of Materials Science and Engineering, College of Electronics and Information Engineering, Institute of Microelectronics, Guangdong Research Center for Interfacial Engineering of Functional Materials, Shenzhen University, Shenzhen 518060, China;

orcid.org/0000-0002-1980-4979; Email: mark_huang@szu.edu.cn

Authors

Xinke Liu – College of Materials Science and Engineering, College of Electronics and Information Engineering, Institute of Microelectronics, Guangdong Research Center for Interfacial Engineering of Functional Materials, Shenzhen University, Shenzhen 518060, China; orcid.org/0000-0002-3472-5945

Jie Zhou – College of Materials Science and Engineering, College of Electronics and Information Engineering, Institute of Microelectronics, Guangdong Research Center for Interfacial Engineering of Functional Materials, Shenzhen University, Shenzhen 518060, China

Jiangliu Luo – College of Materials Science and Engineering, College of Electronics and Information Engineering, Institute of Microelectronics, Guangdong Research Center for Interfacial Engineering of Functional Materials, Shenzhen University, Shenzhen 518060, China

Hangning Shi – State Key Laboratory of Functional Materials for Informatics, Shanghai Institute of Microsystem and Information Technology, Chinese Academy of Sciences, Shanghai 200050, China; Center of Materials Science and Optoelectronics Engineering, University of Chinese Academy of Sciences, Beijing 100049, China

Tiangui You – State Key Laboratory of Functional Materials for Informatics, Shanghai Institute of Microsystem and Information Technology, Chinese Academy of Sciences, Shanghai 200050, China; Center of Materials Science and Optoelectronics Engineering, University of Chinese Academy of Sciences, Beijing 100049, China

Xin Ou – State Key Laboratory of Functional Materials for Informatics, Shanghai Institute of Microsystem and Information Technology, Chinese Academy of Sciences, Shanghai 200050, China; Center of Materials Science and Optoelectronics Engineering, University of Chinese Academy of Sciences, Beijing 100049, China; orcid.org/0000-0002-0316-9958

Venkatadivakar Botcha – College of Materials Science and Engineering, College of Electronics and Information Engineering, Institute of Microelectronics, Guangdong Research Center for Interfacial Engineering of Functional Materials, Shenzhen University, Shenzhen 518060, China

Fengwen Mu – SABers Co., Ltd., Tianjing 300451, China; orcid.org/0000-0001-7396-9347

Tadatomo Suga – Collaborative Research Center, Meisei University, Tokyo 191-8506, Japan

Xinzhong Wang – Information Technology Research Institute, Shenzhen Institute of Information Technology, Shenzhen 518172, China

Complete contact information is available at: <https://pubs.acs.org/10.1021/acsomega.2c05049>

Notes

The authors declare no competing financial interest.

ACKNOWLEDGMENTS

This work was supported by the National Key Research and Development Program of China (2017YFB0403000), National Natural Science Foundation of China (61974144), Guangdong Province Key Research and Development Plan (2020B010174003), the Science and Technology Foundation

of Shenzhen (JSGG20191129114216474), the Science and Technology Project of Shenzhen City (JSGG20210802154213040 and JSGG20201102152403008), and Project of Innovation and Strong School (PT2020C002). The authors wish to acknowledge the assistance on HRTEM observation received from the Electron Microscope Center of the Shenzhen University and device fabrication process in the Photonics Center of Shenzhen University. The Sulfur powder was provided by Xintai Wenhe Chemical Pte Ltd (China, Shandong). The CVD system (CVD-12IIIH-3Z/G) was provided by Tianjin Zhonghuan Furnace Corp. The Open Project of State Key Laboratory of Functional Materials for Informatic.

REFERENCES

- (1) Liu, X. K.; Hu, S. Q.; Luo, J. L.; Li, X. H.; Wu, J.; Chi, D. Z.; Ang, K. W.; Yu, W. J.; Cai, Y. Q. Suspended MoS₂ Photodetector Using Patterned Sapphire Substrate. *Small* **2021**, *17*, 2100246.
- (2) Liu, X. K.; Luo, J. L.; Lin, Y. H.; Lin, Z. C.; Liu, X.; He, J. L.; Yu, W. J.; Liu, Q.; Wei, T. B.; Yang, J. K.; Zhang, W. J.; Guo, J. High-Performance Photodetectors Using a 2D MoS₂/3D-AlN Structure. *ACS Appl. Electron. Mater.* **2021**, *3*, 5415–5422.
- (3) Li, Z. W.; Wu, J.; Wang, C.; Zhang, H.; Yu, W. J.; Lu, Y. M.; Liu, X. K. High-performance monolayer MoS₂ photodetector enabled by oxide stress liner using scalable chemical vapor growth method. *Nanophotonics* **2020**, *9*, 1981–1991.
- (4) Xia, F. N.; Wang, H.; Xiao, D.; Dubey, M.; Ramasubramaniam, A. Two-Dimensional Material Nanophotonics. *Nat. Photonics* **2014**, *8*, 899–907.
- (5) Terrones, M.; Botello-Méndez, A. R.; Campos-Delgado, J.; López-Urías, F.; Vega-Cantú, Y. I.; Rodríguez-Macias, F. J.; Elias, A. L.; Muñoz-Sandoval, E.; Cano-Márquez, A. G.; Charlier, J. C.; Terrones, H. Graphene and graphite nanoribbons: Morphology, properties, synthesis, defects and applications. *Nano Today* **2010**, *5*, 351–372.
- (6) Lam, K. T.; Liang, G. C. An ab initio study on energy gap of bilayer graphene nanoribbons with armchair edges. *Appl. Phys. Lett.* **2008**, *92*, 223106.
- (7) Wang, R. Y.; Xu, X.; Yu, Y. W.; Ran, M.; Zhang, Q. F.; Li, A. J.; Zhuge, F. W.; Li, H. Q.; Gan, L.; Zhai, T. Y. The mechanism of the modulation of electronic anisotropy in two-dimensional ReS₂. *Nanoscale* **2020**, *12*, 8915–8921.
- (8) Hafeez, M.; Gan, L.; Li, H. Q.; Ma, Y.; Zhai, T. Y. Large-Area Bilayer ReS₂ Film/Multilayer ReS₂ Flakes Synthesized by Chemical Vapor Deposition for High Performance Photodetectors. *Adv. Funct. Mater.* **2016**, *26*, 4551–4560.
- (9) Xie, D. D.; Yin, K.; Yang, Z. J.; Huang, H.; Li, X. H.; Shu, Z. W.; Duan, H. G.; He, J.; Jiang, J. Polarization-perceptual anisotropic two-dimensional ReS₂ neuro-transistor with reconfigurable neuromorphic vision. *Mater. Horiz.* **2022**, *9*, 1448–1459.
- (10) Adepou, V.; Bokka, N.; Mattela, V.; Sahatiya, P. A highly electropositive ReS₂ based ultra-sensitive flexible humidity sensor for multifunctional applications. *New J. Chem.* **2021**, *45*, 5855–5862.
- (11) Li, X. B.; Cui, F. F.; Feng, Q. L.; Wang, G.; Xu, X. S.; Wu, J. X.; Mao, N. N.; Liang, X.; Zhang, Z. Y.; Zhang, J.; Xu, H. Controlled growth of large-area anisotropic ReS₂ atomic layer and its photodetector application. *Nanoscale* **2016**, *8*, 18956–18962.
- (12) Zhong, J. H.; Zeng, C.; Yu, J.; Cao, L. K.; Ding, J. N.; Liu, Z. W.; Liu, Y. P. Direct Observation of Enhanced Performance in suspended ReS₂ Photodetectors. *Opt. Express* **2021**, *29*, 3567–3574.
- (13) Lee, S. H.; Park, J.; Choi, S. B.; An, S.; Jung, M.; Seo, J.; Lee, M. J. Photocurrent response in few-layered ReS₂ devices with short and open circuits. *J. Korean Phys. Soc.* **2022**, *80*, 53–58.
- (14) Huang, X. C.; Deng, L. F.; Guo, Z. L.; Luo, N. Q.; Liu, J.; Zhao, Y.; Liu, Z.; Wei, A. X. Layer-dependent electrical transport property of two-dimensional ReS₂ thin films. *J. Mater. Sci.: Mater. Electron.* **2021**, *32*, 24342–24350.

- (15) Zhou, Y.; Meng, X.; Wang, Y. Abnormal Anisotropic Nonlinear Absorption in Bulk ReS₂ Measured by Intensity-scan Method. *2020 Conference on Lasers and Electro-Optics*, 2020, pp 1–2.
- (16) Liu, F. C.; Zheng, S. J.; He, X. X.; Chaturvedi, A.; He, J. F.; Chow, W. L.; Mion, T. R.; Wang, X. L.; Zhou, J. D.; Fu, Q. D.; et al. Highly Sensitive Detection of Polarized Light Using Anisotropic 2D ReS₂. *Adv. Funct. Mater.* **2016**, *26*, 1146.
- (17) Yu, S.; Zhu, H.; Eshun, K.; Shi, C.; Zeng, M.; Li, Q. L. Strain-engineering the anisotropic electrical conductance in ReS₂ monolayer. *Appl. Phys. Lett.* **2016**, *108*, 191901.
- (18) Ho, C. H.; Huang, Y. S.; Tiong, K. K. In-plane anisotropy of the optical and electrical properties of ReS₂ and ReSe₂ layered crystals. *J. Alloys Compd.* **2001**, *317-318*, 222–226.
- (19) Lv, J.; Yang, J. J.; Jiao, S. L.; Huang, P.; Ma, K. J.; Wang, J. Q.; Xu, X. X.; Liu, L. Ultrathin Quasibinary Heterojunctioned ReS₂/MoS₂ Film with Controlled Adhesion from a Bimetallic Co-feeding Atomic Layer Deposition (ALD). *ACS Appl. Mater. Interfaces* **2020**, *12*, 43311–43319.
- (20) Shi, H. N.; Huang, K.; Mu, F. W.; You, T. G.; Ren, Q. H.; Lin, J. J.; Xu, W. H.; Jin, T. T.; Huang, H.; Yi, A. L.; et al. Realization of wafer-scale single-crystalline GaN film on CMOS-compatible Si(100) substrate by ion-cutting technique. *Semicond. Sci. Technol.* **2020**, *35*, 125004.
- (21) Allred, A. L. Electronegativity values from thermochemical data. *J. Inorg. Nucl. Chem.* **1961**, *17*, 215–221.
- (22) Chenet, D. A.; Aslan, O. B.; Huang, P. Y.; Fan, C.; van der Zande, A. M.; Heinz, T. F.; Hone, J. C. In-Plane Anisotropy in Mono- and Few-Layer ReS₂ Probed by Raman Spectroscopy and Scanning Transmission Electron Microscopy. *Nano Lett.* **2015**, *15*, 5667–5672.
- (23) Jena, D.; Simon, J.; Wang, A.; Cao, Y.; Goodman, K.; Verma, J.; Ganguly, S.; Li, G. W.; Karda, K.; Protasenko, V.; et al. Polarization-Engineering in III-V Nitride Heterostructures: New Opportunities For Device Design. *Phys. Status Solidi* **2011**, *208*, 1511–1516.
- (24) Bernardini, F.; Fiorentini, V.; Vanderbilt, D. Spontaneous polarization and piezoelectric constants of III-V nitrides. *Phys. Rev. B: Condens. Matter Mater. Phys.* **1997**, *56*, 10024–10027.
- (25) Wu, Y.; Li, Z. W.; Ang, K. W.; Jia, Y. P.; Shi, Z. M.; Huang, Z.; Yu, W. J.; Sun, X. J.; Liu, X. K.; Li, D. B. Monolithic integration of MoS₂-based visible detectors and GaN-based UV detectors. *Photonics Res.* **2019**, *7*, 1127–1133.
- (26) Hodgson, E. R.; Lambert, R. K.; James. Photoelectric effect. *Phys. Educ.* **1975**, *10*, 123–124.
- (27) Christensen, O. Quantum efficiency of the internal photoelectric effect in silicon and germanium. *J. Appl. Phys.* **1976**, *47*, 689–695.
- (28) Pratt, R. H. Atomic Photoelectric Effect at High Energies. *Phys. Rev.* **1960**, *117*, 1017–1028.
- (29) Das, K.; Samanta, S.; Kumar, P.; Narayan, K. S.; Raychaudhuri, A. K. Fabrication of Single Si Nanowire Metal–Semiconductor–Metal Device for Photodetection. *IEEE Trans. Electron Devices* **2014**, *61*, 1444–1450.
- (30) Gabor, N. M.; Zhong, Z. H.; Bosnick, K.; McEuen, P. L. Ultrafast Photocurrent Measurement of the Escape Time of Electrons and Holes from Carbon Nanotube p-i-n Photodiodes. *Phys. Rev. Lett.* **2011**, *108*, 087404.
- (31) Zhang, W. J.; Huang, J. K.; Chen, C. H.; Chang, Y. H.; Cheng, Y. J.; Li, L. J. High-Gain Phototransistors Based on a CVD MoS₂ Monolayer. *Adv. Mater.* **2013**, *25*, 3456–3461.
- (32) Mouri, S.; Miyauchi, Y.; Toh, M.; Zhao, W. J.; Eda, G.; Matsuda, K. Nonlinear photoluminescence in atomically thin layered WSe₂ arising from diffusion-assisted exciton-exciton annihilation. *Phys. Rev. B: Condens. Matter Mater. Phys.* **2014**, *90*, 155449.
- (33) Li, L. A.; Liu, Z. C.; Wang, L.; zhang, B. J.; Liu, Y.; Ao, J. P. Self-powered GaN ultraviolet photodetectors with p-NiO electrode grown by thermal oxidation. *Mater. Sci. Semicond. Process.* **2018**, *76*, 61–64.